Development of an Omnidirectional Modular Robot

Fernando Lucio-Reyna, Ricardo Tapia-Herrera, *Member, IEEE*, Tonatiuh Hernández-Cortés, Israel Lizardo-Parra, and Jesús A. Meda-Campaña, *Senior Member, IEEE*

***Abstract*—The concept of modularity in mobile robots has been aimed to enhance their capabilities, including functionality, adaptability, or robustness. However, modularity often involves the complex design of robotic modules. In this context, this paper introduces the development of a reconfigurable modular mobile robot in differential drive configuration, which main advantage is the generation of an omnidirectional mobile robot when at least two modules are coupled, in consequence, mobility and load capacity are increased. Each robotic module comprises a frame, two Mecanum wheels, a controller, and an active connection mechanism designed to simultaneously perform two functions: 1) locking a module-to-module connection, and 2) automatic reconfiguration of the robot's architecture by lifting a freely rotating spherical wheel. Owing to the integration of Mecanum wheels, the kinematic analysis of differential drive configuration considers the influence of a rollers' angles relative to the robot frame, allowing the model to be extended to a system with n coupled modules. To validate the kinematic models, a multibody simulation was conducted using Simscape Multibody Link™. Finally, a prototype is presented to showcase the modularity capability, including the docking and undocking process, as well as the omnidirectional mobility, even in the presence of backlash.**

Link to graphical and video abstracts, and to code: https://latamt.ieeer9.org/index.php/transactions/article/view/9673

***Index Terms*—Omnidirectional robot, modular robot, mobile robot, kinematics, mecanum wheels**

I. Introduction

MODULAR robots are systems with enhanced and extended functionalities resulting from the combination of simple robotic modules capable of reconfiguring themselves into different arrangements. Modular robotic systems (MRS) can perform tasks that individual modules are unable to accomplish independently. The modules in an MRS can be classified as homogeneous if they possess the same characteristics in terms of functionality, geometric design, processing capabilities, and power supply. If any of the above conditions are not met, the modules are considered nonhomogeneous [1]. Additionally, in [2] is proposed a classification based on the geometric configuration of modules, which includes lattice, chain, and mobile architectures.

Omnidirectional robots have the capability to move in any planar direction without changing the orientation of its chassis or wheels [3]. When omnidirectional and modularization concepts are combined, novel drive configurations can emerge. This concept was introduced in [4] and later explored by [5], where are proposed robotic modules that employs either standard or Mecanum wheels to form new configurations when they are coupled. In [6], an active tractor-trailer system is designed, with two standard wheels for the tractor and two nonpowered Mecanum wheels for the trailer module. Davis et al. [7], [8] propose a modular system that forms a holonomic drive with three omnidirectional wheels focused to develop cooperative tasks and self-repair. Similarly, in [9] is designed an omnidirectional modular robot based on omni-wheels and active docking mechanisms, this robot is capable of performing self-repair while the robot group maintains collective motion. Yunwang et al. in [10]–[12] propose and analyze the omnidirectional mobility of multiple configurations resulting from different connection types between individual robots, such as end to end, side by side, symmetrical-rectangular, and distributed combination.

The reconfiguration of omnidirectional robotic platforms has been a topic of interest in research, due to advancements in technological tools. In this context, for four-wheel Mecanum robots, two configurations are commonly used: Type-X and Type-O [13]. However, researches as [14], [15] demonstrate the possibility of reconfiguring the chassis of four-wheel Mecanum robots from the Type-X configuration to a four-in-line arrangement, to accomplish exploration tasks in narrow areas. A similar concept is introduced in [16], where are studied the motion performance and transformation process between I shape and C shape of a robotic omnidirectional platform. In [17] is designed and analyzed an omnidirectional reconfigurable wheeled robot capable of switching between omnidirectional and conventional wheeled modes to perform holonomic movements over inclined surfaces and achieve energy-efficient movements. Likewise, [18] proposes a drive model that adjusts the wheel spacing between omnidirectional drives, allowing reconfiguration and omnidirectional mobility simultaneously. Parween et al. [19] present an interesting concept of a differential mobile robot capable to reconfigure the position of its drives to navigate through different areas, although it lacks omnidirectional motion. Additionally, Karamipour et al. [20] presented the design, analysis, and simulation of a reconfigurable mobile robot characterized by adjusting the chassis width and length through specific motion modes of its omnidirectional wheels. Moreover, industrial applications have been developed by Kuka Robotics with the design of omnidirectional drive technology [21].

Modularization of omnidirectional robots has been explored generally when they are fully assembled to perform holonomic

The associate editor coordinating the review of this manuscript and approving it for publication was Javier Moreno-Valenzuela (*Corresponding author: Ricardo Tapia-Herrera*).

F. Lucio-Reyna, Ricardo Tapia-Herrera, I. Lizardo-Parra, and J. A. Meda-Campana are with the National Polytechnic Institute, México City, México (e-mails: flucior0900@alumno.ipn.mx, rtapiah@ipn.mx, ilizardop2100@alumno.ipn.mx, and jmedac@ipn.mx).

T. Hernández-Cortés is with Mechatronics Institute, Polytechnic University of Pachuca, Hidalgo, México (e-mail: tonatiuh@upp.edu.mx).

motion. In contrast, this paper proposes the development of nonhomogeneous modular mobile robots in differential drive configuration using Mecanum wheels. These modules have the capability to connect with each other, to generate an omnidirectional mobile robot, in consequence its load capacity and mobility will increase. The proposed robot possesses the characteristic of reconfiguration, which is achieved when individual modules are coupled through an active connection mechanism. Owing to the integration of Mecanum wheels, the kinematic analysis of differential drive configuration considers the influence of a rollers' angles relative to the robot frame, allowing the model to be extended to a system with n coupled modules.

The article is organized as follows: Section 2 describes the conceptual design of the modules and their coupled configuration. Section 3 presents the kinematic analysis based on the determination of the inverse Jacobian matrix. In Section 4 are performed numerical simulations using Simscape Multibody Link™ software, and the prototype is introduced. Finally, conclusions are given in Section 5.

II. Methodology

The proposed robot is based on the concepts of reconfiguration and modularity, which imply variations in its structure, particularly in its type of locomotion. From a kinematic perspective, changes in locomotion require modeling the robot in differential drive configuration, under the assumption that this model can be extended to other configurations derived from the connection of multiple modules. Therefore, subsequent sections describe the proposed platform, its operation, and the mathematical concepts used to model the robot.

A. Platform Description

As shown in Fig. 1, the proposed architecture consists of two nonhomogeneous mobile robots in differential drive configuration. Each module comprises a main frame, a power supply system, a controller (Arduino Nano ®), two micro gear motors with a peak torque of 2 kg-cm at 30 rpm (298:1 ratio), an active connection mechanism, a spherical wheel that brings stability to the robotic module, and male/female connectors. In individual mode, modules exhibit the characteristic motion of differential drive robots, i.e. forward/backward movement and rotation. However, due to their nonholonomic nature, modules cannot move directly sideways. This limitation is overcome when at least two modules are connected, because Modules I and II incorporate Type A-B Mecanum wheels arranged in opposite orientations, in which case the system behaves as a holonomic robot.

B. Connection Mechanism and Modules Reconfiguration

Different designs of interlocking mechanisms have been proposed to reduce the misalignment and offsets, such as using plates with locking fingers [26], retracting hooks [27], pin-hole systems [28], or adapting mechanisms [29]. The choice of a connection mechanism will depend of the specific application of the Modular Robotic System (MRS), the allowable tolerances, and the coupling/decoupling strategies. For the proposed robot, modules achieve automatic reconfiguration through the implementation of the active mechanism that enables a quick and secure coupling between modules under the pin-hole principle. As shown in Fig. 2, the mechanism comprises: a) a latch arm rigidly connected to a spherical wheel, b) a servomotor that rotates the latch arm ± 53, and c) a set of male/female connectors.

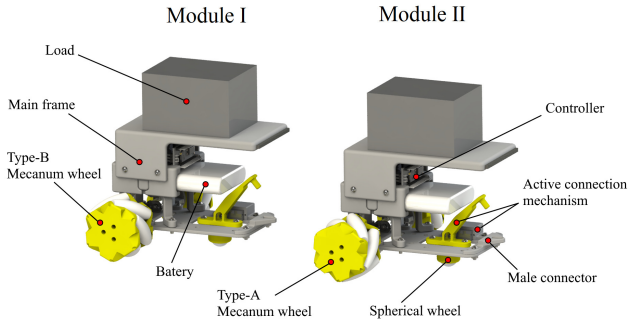

Fig. 1. Omnidirectional modular robot concept.

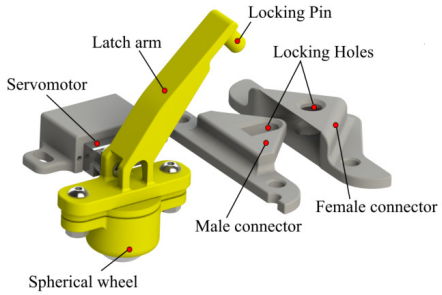

Fig. 2. Detailed view of the active connection mechanism.

For coupling, the modules in a differential drive configuration must approach one behind the other with the same orientation, which allows proper alignment of the male and female connectors. As shown in Fig. 3, the reconfiguration from differential drive to omnidirectional robot occurs once the male connector is inserted into the female connector. Subsequently, the servomotor rotates the latch arm 53° clockwise, inserting the arm's pin into the locking holes. Simultaneously, the arm lifts the spherical wheel a distance s to prevent ground interference during omnidirectional operation, this condition must be met in both modules. During decoupling, rotating the latch arm 53° counterclockwise unlocks the modules and at same time lowers the spherical wheel, restoring stability in differential drive mode and enabling reconfiguration from omnidirectional to differential locomotion.

C. Kinematics

The kinematic analysis of the module considers characteristics such as the number of wheels, its geometric arrangement of the wheels, and the angles of the rollers relative to the robot frame. Additionally, it is assumed that the spherical wheel

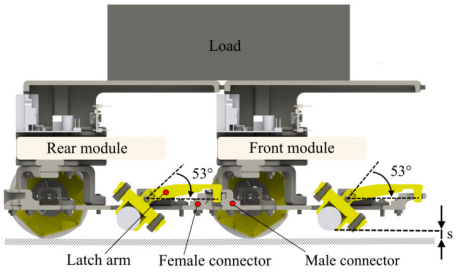

Fig. 3. Section view when two modules are coupled

does not induce any interference or restrictions to the robot's motion.

D. Kinematics for Differential Drive Configuration

The velocity vectors are shown in Fig. 4, where R represents center of rotation in differential drive configuration, and (x_R, y_R) defines the local reference frame of the robot. Axes E_i and S_i correspond to the local reference frames of the wheels $i = 1, 2$, d is the distance from origin R to the center of the wheel O_i along the y_R direction. The total velocity at each wheel, V_{Rir}, is decomposed into the tangential component due to the wheel rotation V_{Ri}, and the component due to the roller rotation V_{ri} at the contact points O_i. It is assumed that there is no slip between the contact points O_i and the ground. Finally, ω is the angular velocity of the module about z_R axis.

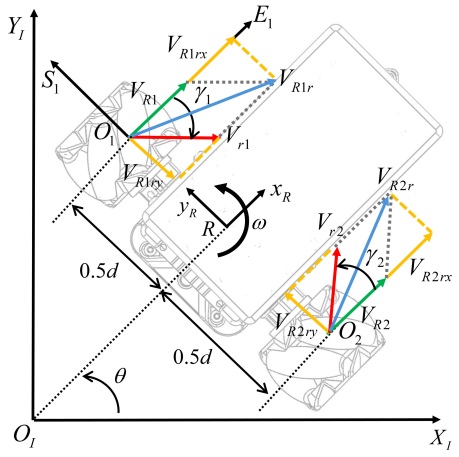

Fig. 4. Coordinate systems and velocity vectors for differential drive configuration.

According to [30], for a Mecanum wheel, the posture kinematic model with respect to the reference frame I, is given by the following expression:

$$\begin{bmatrix} c(\beta_i - \gamma_i) & s(\beta_i - \gamma_i) & l_i s(\beta_i - \gamma_i - \alpha_i) \end{bmatrix} {}^R\dot{\xi} = -r\dot{\varphi}_i s(\gamma_i) \quad (1)$$

Here, $s = sin$, $c = cos$, r is the radius of the wheels, $\dot{\varphi}_i$ is the angular velocity of the wheel i about its own rotation axis, l_i and α_i define the position of the origin O_i with respect to the robot frame R, β_i is the angle between S_i and x_R, and γ_i is the angle of the rollers relative to the wheel plane. The velocities in the local robot frame are given by ${}^R\dot{\xi} = [\dot{x}_R, \dot{y}_R, \omega]^T$, such that ${}^I\dot{\xi} = {}^I R_R {}^R\dot{\xi}$, where ${}^I R_R$ is the rotation matrix that transforms the velocities from local frame R to the global reference frame I. Consequently, for each module, it is possible to express its inverse kinematics from equation 1 in the following form:

$$\begin{bmatrix} \dot{\varphi}_1 \\ \dot{\varphi}_2 \end{bmatrix} = -\frac{1}{r} \begin{bmatrix} \frac{c(\beta_1-\gamma_1)}{s(\gamma_1)} & \frac{s(\beta_1-\gamma_1)}{s(\gamma_1)} & \frac{l_1 s(\beta_1-\gamma_1-\alpha_1)}{s(\gamma_1)} \\ \frac{c(\beta_2-\gamma_2)}{s(\gamma_2)} & \frac{s(\beta_2-\gamma_2)}{s(\gamma_2)} & \frac{l_2 s(\beta_2-\gamma_2-\alpha_2)}{s(\gamma_2)} \end{bmatrix} {}^R\dot{\xi}, \quad (2)$$

equation (2) is expressed in terms of the inverse Jacobian matrix as follows:

$$\begin{bmatrix} \dot{\varphi}_1 \\ \dot{\varphi}_2 \end{bmatrix} = \mathbf{J}^{-1} \begin{bmatrix} \dot{x}_R & \dot{y}_R & \omega \end{bmatrix}^T, \quad (3)$$

with:

$$\mathbf{J}^{-1} = -\frac{1}{r} \begin{bmatrix} \frac{c(\beta_1-\gamma_1)}{s(\gamma_1)} & \frac{s(\beta_1-\gamma_1)}{s(\gamma_1)} & \frac{l_1 s(\beta_1-\gamma_1-\alpha_1)}{s(\gamma_1)} \\ \frac{c(\beta_2-\gamma_2)}{s(\gamma_2)} & \frac{s(\beta_2-\gamma_2)}{s(\gamma_2)} & \frac{l_2 s(\beta_2-\gamma_2-\alpha_2)}{s(\gamma_2)} \end{bmatrix} \quad (4)$$

The direct kinematics of the module can be obtained using the Moore-Penrose pseudoinverse. That is, if $\mathbf{J}^{-1} \in \mathbb{R}^{m \times n}$ with $m < n$ and $\mathbf{J}^{-1} = A$, then $\mathbf{J} = A^T(AA^T)^{-1}$, consequently the velocities for the differential drive configuration are expressed in the local frame R by:

$${}^R\dot{\xi} = \mathbf{J} \begin{bmatrix} \dot{\varphi}_1 & \dot{\varphi}_2 \end{bmatrix}^T \quad (5)$$

E. Kinematics of k and $k+1$ Modules Connection

Based on (1), the kinematics of the coupled robot can be obtained by considering that point R is located at the new geometric center a distance $0.5d$ due to the connection between modules k and $k+1$. As shown in Fig. 5 the axes $E_{i,k}, S_{i,k}$ with origin at $O_{i,k}$ are associated with each wheel i of module k. Therefore, the inverse Jacobian in a system of n modules is constructed as:

$$\mathbf{J}^{-1} = -\frac{1}{r} \begin{bmatrix} \frac{c(\beta_{1,1}-\gamma_{1,1})}{s(\gamma_{1,1})} & \frac{s(\beta_{1,1}-\gamma_{1,1})}{s(\gamma_{1,1})} & \frac{l_{1,1} s(\beta_{1,1}-\gamma_{1,1}-\alpha_{1,1})}{s(\gamma_{1,1})} \\ \frac{c(\beta_{2,1}-\gamma_{2,1})}{s(\gamma_{2,1})} & \frac{s(\beta_{2,1}-\gamma_{2,1})}{s(\gamma_{2,1})} & \frac{l_{2,1} s(\beta_{2,1}-\gamma_{2,1}-\alpha_{2,1})}{s(\gamma_{2,1})} \\ \vdots & \vdots & \vdots \\ \frac{c(\beta_{2,n}-\gamma_{2,n})}{s(\gamma_{2,n})} & \frac{s(\beta_{2,n}-\gamma_{2,n})}{s(\gamma_{2,n})} & \frac{l_{2,n} s(\beta_{2,n}-\gamma_{2,n}-\alpha_{2,n})}{s(\gamma_{2,n})} \end{bmatrix} \quad (6)$$

Finally, the i, n wheel velocities are obtained from:

$$\begin{bmatrix} \dot{\varphi}_{1,1} \\ \dot{\varphi}_{2,1} \\ \vdots \\ \dot{\varphi}_{2,n} \end{bmatrix} = \mathbf{J}^{-1} {}^R\dot{\xi} \quad (7)$$

Under the assumption that in (6) $m > n$, it follows that the Jacobian matrix can be expressed as $\mathbf{J} = (A^T A)^{-1} A^T$, with $A = \mathbf{J}^{-1}$. Consequently, the robot's velocities in the inertial reference frame I are given by:

$${}^I\dot{\xi} = \begin{bmatrix} Vx \\ Vy \\ \omega \end{bmatrix} = {}^I R_R \, \mathbf{J} \begin{bmatrix} \dot{\varphi}_{1,1} \\ \dot{\varphi}_{2,1} \\ \vdots \\ \dot{\varphi}_{2,n} \end{bmatrix} \quad (8)$$

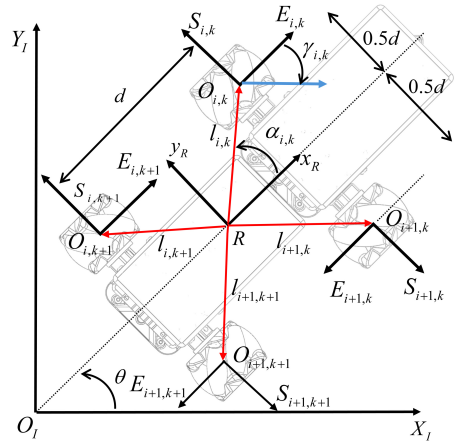

Fig. 5. Coordinate systems and velocity vectors due to the wheels mounted on the chassis when modules k and $k+1$ are connected.

where:

$$ {}^{I}R_R = \begin{bmatrix} c(\theta) & -s(\theta) & 0 \\ s(\theta) & c(\theta) & 0 \\ 0 & 0 & 1 \end{bmatrix} \tag{9} $$

III. Case of Study

As mentioned above, due to the wheels arrangement, the modules are nonhomogeneous, resulting in different Jacobian matrix for each module. For Module I, are considered the following parameters: $l_1 = l_2 = d = 66\ mm$, $r = 27\ mm$, $\alpha_1 = 180$, $\alpha_2 = 0$, $\beta_1 = -180$, $\beta_2 = 0$, $\gamma_1 = -45$, $\gamma_2 = 45$. For Module II the parameters are: $l_1 = l_2 = d$, $\alpha_1 = 180$, $\alpha_2 = 0$, $\beta_1 = -180$, $\beta_2 = 0$, $\gamma_1 = 45$, $\gamma_2 = -45$. The inverse kinematics for Modules I and II is then given respectively, as:

$$ \begin{bmatrix} \dot{\varphi}_1 \\ \dot{\varphi}_2 \end{bmatrix}_I = -\frac{1}{r} \begin{bmatrix} -1 & 1 & \sqrt{2}d \\ 1 & 1 & \sqrt{2}d \end{bmatrix}_I {}^{R}\dot{\xi}_I \tag{10} $$

$$ \begin{bmatrix} \dot{\varphi}_1 \\ \dot{\varphi}_2 \end{bmatrix}_{II} = -\frac{1}{r} \begin{bmatrix} -1 & -1 & \sqrt{2}d \\ 1 & -1 & \sqrt{2}d \end{bmatrix}_{II} {}^{R}\dot{\xi}_{II} \tag{11} $$

For a four-wheel Mecanum robot, the parameters are defined as follows: $\alpha_{1,1} = 45$, $\alpha_{2,1} = -45$, $\alpha_{1,2} = 135$, $\alpha_{2,2} = -135$, $\beta_{1,1} = \beta_{1,2} = -90$, $\beta_{2,1} = \beta_{2,2} = 90$, $\gamma_{1,1} = \gamma_{2,2} = -45$ and $\gamma_{2,1} = \gamma_{1,2} = 45$, $l_{1,1} = l_{2,1} = l_{1,2} = l_{2,2} = 2\sqrt{d}$. Substituting these values into (6) and (7), the angular velocities of the wheels are:

$$ \begin{bmatrix} \dot{\varphi}_{1,1} \\ \dot{\varphi}_{2,1} \\ \dot{\varphi}_{1,2} \\ \dot{\varphi}_{2,2} \end{bmatrix} = -\frac{1}{r} \begin{bmatrix} 1 & 1 & -2d \\ -1 & 1 & 2d \\ -1 & 1 & -2d \\ 1 & 1 & 2d \end{bmatrix} \dot{\xi}_R \tag{12} $$

In the case of a six-wheel Mecanum robot, the parameters are defined as follows: $\alpha_{1,1} = 26.57$, $\alpha_{2,1} = -26.57$, $\alpha_{1,2} = 90$, $\alpha_{2,2} = -90$, $\alpha_{1,3} = 153.43$, $\alpha_{2,3} = -153.43$, $\beta_{1,1} = \beta_{1,2} = \beta_{1,3} = -90$, $\beta_{2,1} = \beta_{2,2} = \beta_{2,3} = 90$, $\gamma_{1,1} = -45$, $\gamma_{2,1} = 45$, $\gamma_{1,2} = -45$, $\gamma_{2,2} = 45$, $\gamma_{1,3} = 45$, $\gamma_{2,3} = -45$, $l_{1,1} = l_{2,1} = \sqrt{d^2 + (0.5d)^2}$, $l_{1,2} = l_{2,2} = 0.5d$, $l_{1,3} = l_{2,3} = \sqrt{d^2 + (0.5d)^2}$. Substituting these parameters into the kinematic equations, yields:

$$ \begin{bmatrix} \dot{\varphi}_{1,1} \\ \dot{\varphi}_{2,1} \\ \dot{\varphi}_{1,2} \\ \dot{\varphi}_{2,2} \\ \dot{\varphi}_{1,3} \\ \dot{\varphi}_{2,3} \end{bmatrix} = -\frac{1}{r} \begin{bmatrix} -1 & 1 & 0.5d + d \\ 1 & 1 & 0.5d + d \\ -1 & 1 & 0.5d \\ 1 & 1 & 0.5d \\ -1 & -1 & 0.5d + d \\ 1 & -1 & 0.5d + d \end{bmatrix} \dot{\xi}_R \tag{13} $$

Last case considers the connection between four modules, the parameters to consider are: $\alpha_{1,1} = 18.43$, $\alpha_{2,1} = -18.43$, $\alpha_{1,2} = 45$, $\alpha_{2,2} = -45$, $\alpha_{1,3} = 135$, $\alpha_{2,3} = -135$, $\alpha_{1,4} = 161.57$, $\alpha_{2,4} = -161.57$, $\beta_{1,1} = \beta_{1,2} = \beta_{1,3} = \beta_{1,4} = -90$, $\beta_{2,1} = \beta_{2,2} = \beta_{2,3} = \beta_{2,4} = 90$, $\gamma_{1,1} = -45$, $\gamma_{2,1} = 45$, $\gamma_{1,2} = -45$, $\gamma_{2,2} = 45$, $\gamma_{1,3} = 45$, $\gamma_{2,3} = -45$, $\gamma_{1,4} = 45$, $\gamma_{2,4} = -45$, $l_{1,1} = l_{2,1} = \sqrt{(0.5d)^2 + (0.5d + d)^2}$, $l_{1,2} = l_{2,2} = 0.5\sqrt{2}d$, $l_{1,3} = l_{2,3} = 0.5\sqrt{2}d$, $l_{1,4} = l_{2,4} = \sqrt{(0.5d)^2 + (0.5d + d)^2}$, resulting:

$$ \begin{bmatrix} \dot{\varphi}_{1,1} \\ \dot{\varphi}_{2,1} \\ \dot{\varphi}_{1,2} \\ \dot{\varphi}_{2,2} \\ \dot{\varphi}_{1,3} \\ \dot{\varphi}_{2,3} \\ \dot{\varphi}_{1,4} \\ \dot{\varphi}_{2,4} \end{bmatrix} = -\frac{1}{r} \begin{bmatrix} -1 & 1 & 2d \\ 1 & 1 & 2d \\ -1 & 1 & d \\ 1 & 1 & d \\ -1 & -1 & d \\ 1 & -1 & d \\ -1 & -1 & 2d \\ 1 & -1 & 2d \end{bmatrix} \dot{\xi}_R \tag{14} $$

IV. Simulations and Results

To validate the kinematic models, numerical simulations were carried out. The analytical models based on (7) and (8) were programmed in MATLAB Simulink™, while multibody simulations were developed using Simscape Multibody Contact Forces Library™. For multibody simulations, four simulation scenarios are proposed: 1) differential drive configuration (Fig. 6a); 2) four-wheeled robot (Fig. 6b); 3) three connected modules (Fig. 6c), and 4) four coupled modules (Fig. 6d). In each scenario, the contacts between the rollers and the fixed element (ground) were established. It is important to mention that each roller has free relative rotational motion with respect to the covers of the Mecanum wheels (yellow elements). Furthermore, the spherical wheel of the active connection mechanism is also in contact with the ground. The Simulink™ simulation uses the ode4 Runge-Kutta numerical method. Constant parameters for wheel radius r and distance d were set to $r = 27.3$ mm and $d = 66$ mm.

A. Simulation Results

As first simulation scenario is proposed a single module executing the following routine: 1) $\dot{x}_R = 80\ mm/s$, $\dot{y}_R = 0\ mm/s$, $\omega = 0.3\ rad/s$, 2) $\dot{x}_R = 80\ mm/s$, $\dot{y}_R = 0\ mm/s$, $\omega = 0\ rad/s$, 3) $\dot{x}_R = 0\ mm/s$, $\dot{y}_R = 0\ mm/s$, $\omega = -0.3\ rad/s$, and 4) $\dot{x}_R = -80\ mm/s$, $\dot{y}_R = 0\ mm/s$, $\omega = 0\ rad/s$. Fig. 7(a) and 7(b) display the displacement of point R in the X_I, Y_I plane. Despite the presence of an error, the paths traced by the multibody and analytical models are similar. The error along axes X_I is $RMSE = 8.7312\ mm$ and Y_I is $RMSE = 20.1492$. It is observed in Fig. 7(c) and Fig.

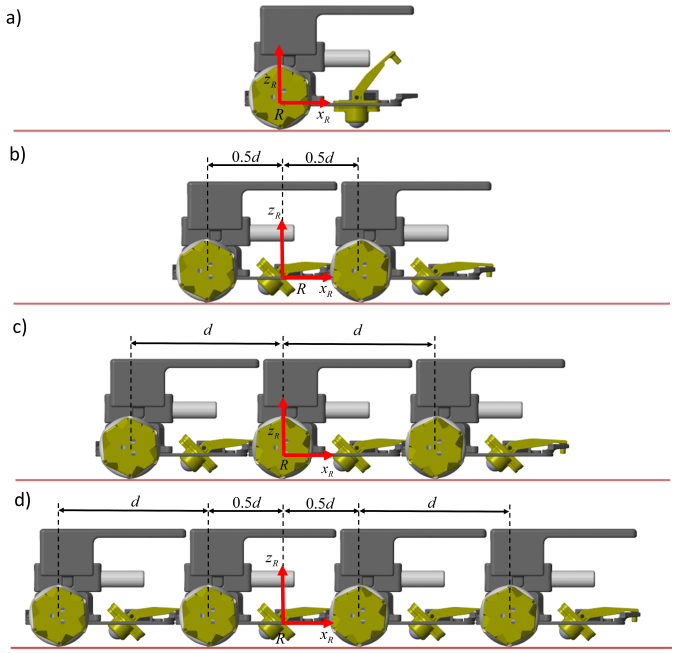

Fig. 6. Multibody simulation scenarios: (a) differential drive configuration, (b) four-wheeled robot, (c) three modules coupled, and (d) four modules coupled.

7(d) that linear and angular velocities fluctuate around their reference values. The corresponding RMSE values for Vx, Vy, ω and θ are: 2.7257 mm/s, 3.7885 mm/s, 0.0305 rad/s and 0.0398 rad, respectively.

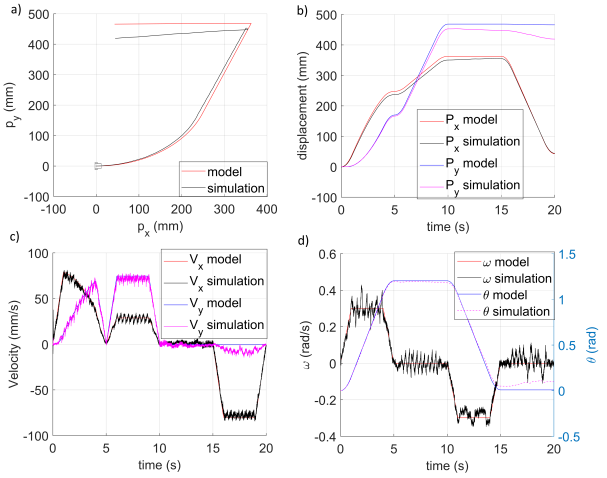

Fig. 7. Simulation results of a single module: (a) trajectory in the X_I, Y_I coordinate frame, (b) displacement along X_I, Y_I axes, (c) robot velocities along X_I, Y_I axes, (d) angular velocity and orientation angle of module around Z_I axis.

In the second simulation scenario, a four wheeled Mecanum robot integrated by two modules is proposed to execute the following routine: 1) $\dot{x}_R = 0\ mm/s$, $\dot{y}_R = 120\ mm/s$, $\omega = -0.45\ rad/s$, 2) $\dot{x}_R = 120\ mm/s$, $\dot{y}_R = 60\ mm/s$, $\omega = 0\ rad/s$, 3) $\dot{x}_R = 0\ mm/s$, $\dot{y}_R = 120\ mm/s$, $\omega = 0\ rad/s$, and 4) $\dot{x}_R = 0\ mm/s$, $\dot{y}_R = 0\ mm/s$, $\omega = 0.45\ rad/s$. As in the previous case, there is a variation between the paths obtained from the analytical and multibody models (Fig. 8(a) and Fig. 8(b)). The RMSE values along X_I and Y_I axes are 72.55 mm and 24.79 mm. Fig. 8(c) and Fig. 8(d) illustrate the behavior of angular velocity and orientation, with a RMSE of 0.0306 rad/seg and 0.0541 rad, respectively.

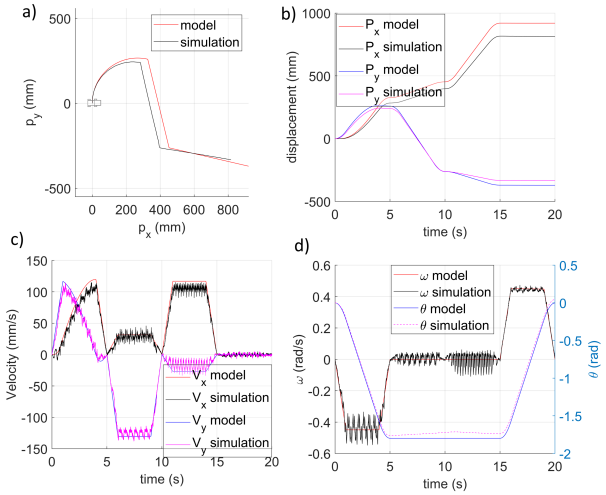

Fig. 8. Simulation results of two modules coupled: (a) trajectory on the X_I, Y_I coordinate frame, (b) displacement along X_I, Y_I axes, (c) robot velocities along X_I, Y_I axes, (d) angular velocity and orientation angle around Z_I axis.

For the case of three modules coupled the routine to execute is: 1) rotation around z_R axis ($\dot{x}_R = 0\ mm/s$, $\dot{y}_R = 0\ mm/s$, $\omega = -0.45\ rad/s$), 2) displacement along y_R ($\dot{x}_R = 0\ mm/s$, $\dot{y}_R = 120\ mm/s$, $\omega = 0\ rad/s$), 3) simultaneous displacement along x_R and y_R axes ($\dot{x}_R = 120\ mm/s$, $\dot{y}_R = 15\ mm/s$, $\omega = 0.45\ rad/s$), and 4) displacement along x_R axis ($\dot{x}_R = 120\ mm/s$, $\dot{y}_R = 0\ mm/s$, $\omega = 0\ rad/s$). Fig. 9(a) and Fig. 9(b) depict the path traced by the six-wheeled robot, presenting RMSE values of 32.47 mm along X_I axis, and 57.74 mm along Y_I axis. Fig. 9(c) and Fig. 9(d) present the obtained linear and angular velocities, as well as the angle θ where the RMSE values are: 8.67 mm/s, 11.91 mm/s, 0.027 rad/s and 0.13 rad.

A final simulation was carried out to compare motion of four coupled modules producing omnidirectional motion. The proposed routine is the following: 1) translation along y_R ($\dot{x}_R = 0\ mm/s$, $\dot{y}_R = 120\ mm/s$, $\omega = 0\ rad/s$), 2) translation along x_R ($\dot{x}_R = 120\ mm/s$, $\dot{y}_R = 0\ mm/s$, $\omega = 0\ rad/s$), 3) rotation around x_R ($\dot{x}_R = 0\ mm/s$, $\dot{y}_R = 0\ mm/s$, $\omega = -0.45\ rad/s$), and 4) simultaneous translation along x_R,y_R, and rotation around z_R ($\dot{x}_R = 120\ mm/s$, $\dot{y}_R = 15\ mm/s$, $\omega = -0.45\ rad/s$). The comparative between the traced paths of analytical and multibody models is depicted in Fig. 10(a) and Fig. 10(b), exhibiting RMSE values of 32.47 mm in X_I and 57.74 mm in Y_I. The corresponding linear and angular velocities are presented in Fig. 10(c) and Fig. 10(d), with RMSE values of 3.6488 mm/s, 7.0566 mm/s, 0.0173 rad/seg and 0.0364 rad

Despite the observed errors, there is similarity between the data obtained from analytical and multibody models. This indicates that the proposed kinematic model can be used

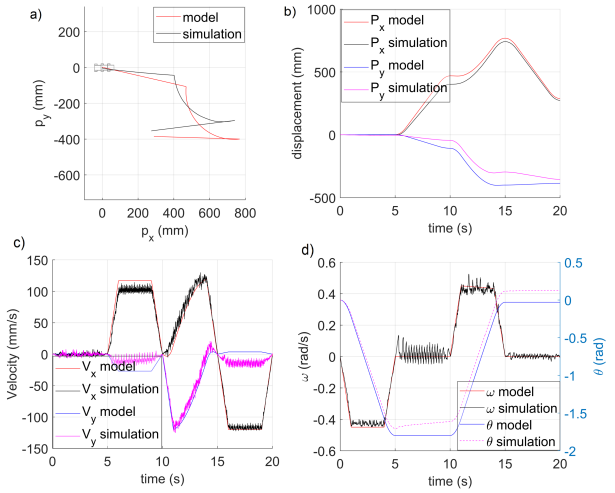

Fig. 9. Simulation results of three modules coupled: (a) traced path in the X_I, Y_I coordinate frame, (b) displacement along X_I, Y_I axes, (c) robot velocities along X_I, Y_I axes, (d) angular velocity and orientation angle around Z_I axis.

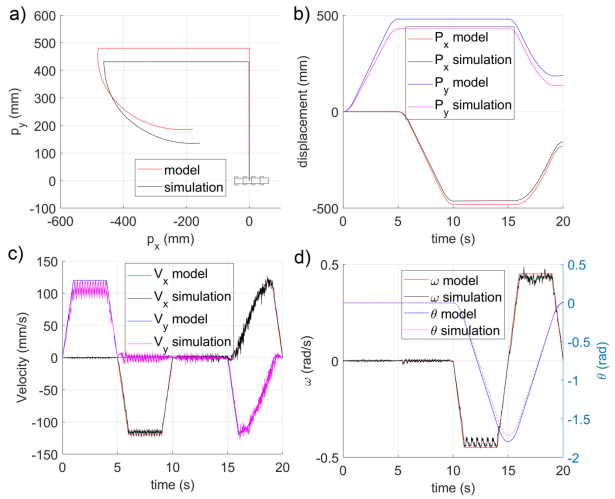

Fig. 10. Simulation results of four modules coupled: (a) trajectory on the X_I, Y_I coordinate frame, (b) displacement along X_I, Y_I axes, (c) robot velocities along X_I, Y_I axes, (d) angular velocity and orientation angle around Z_I axis.

for control design purposes and trajectory planning. On the other hand, the existence of the error can be attributed to some factors that kinematic model does not consider but multibody model does, such as inertia, friction, and wheel geometry that induces oscillations in the modules due to the impact of rollers against the ground. Additionally, geometry of connectors was designed to avoid or reduce the misalignment between the k and $k+1$ modules, but real prototype present backlash inherent to tolerances, and manufacturing process. This backlash produces relative rotation between modules around connection axis, resulting in orientation errors that increase with the number of connected modules. To avoid mechanical modifications, these errors could be minimized with the appropriate control scheme. Therefore, it is necessary to have a dynamic model that considers these factors for a better representation of the system.

B. Prototype Construction

In Fig. 11 is depicted a prototype, which was manufactured using a feasible, cost-effective and straightforward manufacturing process. The prototype was printed in PLA, with a weight of 1.250 kg when it is coupled. Its dimensions are 278.5 mm in length, 176 mm in width and 95 mm in height. Each prototype integrates an Arduino Nano™, which has the inputs and outputs required. Two output pins are employed for PWM (1 PWM output for each motor) for speed control. The DC motors are controlled by the L298N driver, for communication, wireless has been adopted, each module has HC-06 Bluetooth devices, operating as slaves once paired with a master Bluetooth device e.g. smart-phone (Fig. 12).

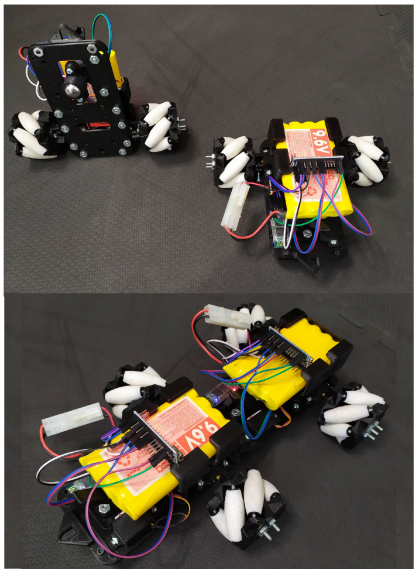

Fig. 11. Real prototype: two single modules (top), and two coupled modules (bottom).

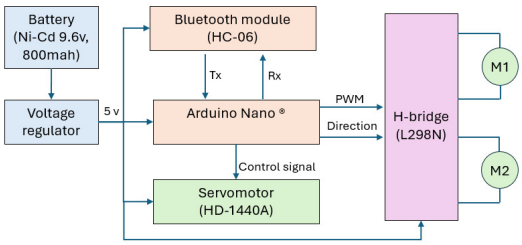

Fig. 12. Electronic architecture for each module

To evaluate the robot's performance, different tests were conducted, focusing on the coupling process, omnidirectional motion, and the decoupling phase. Video frames of these tests are shown in Fig. 13 green arrow indicates the direction of movement. During the coupling process, the connection mechanism accurately aligns both modules(frames 1-3), followed by the rotation of the latch arm to complete the coupling (frame 4). Once the coupling is achieved, omnidirectional behavior is demonstrated (frames 5-13). The decoupling process, shown

TABLE I
COMPARATIVE OF FEATURES OF MODULAR AND RECONFIGURABLE WHEELED ROBOTS

	Modularity	Module locomotion	Coupled Locomotion	Module Reconfiguration	Connection Mechanism	Actuators for Locomotion
Hofbaur et al. [4]	Unit drives	—	Omnidirectional by Mecanum or steered wheels	—	Active	2 per unit
Tatar and Cirebea [5]	Unit drives	—	Differential drive, omnidirectional, combined	—	Manual	1 or 2 per unit
Liu et al. [6]	—	—	Active articulated tractor-trailer	—	—	3
Davis et al. [8]	Unit drives	—	Omnidirectional by omni-wheels	—	Active	1 per unit
Peck et al. [9]	Differential modules	Differential by omni-wheels	Omnidirectional by omni-wheels	—	Active	2 per module
Li et al. [10]	Mecanum modules	Omnidirectional	Omnidirectional	—	Manual	4 per module
Pasumarthi et al. [12]	Mecanum modules	Omnidirectional	Omnidirectional	—	Active	4 per module
He et al. [13]	—	Omnidirectional	—	Type X, Type O	—	4 per module
Li et al. [14]	—	Omnidirectional	—	car, snake	—	4 per module
Cheah et al. [14]	—	Omnidirectional	—	car, snake	—	4 per module
Chi et al. [16]	—	Omnidirectional	—	I Shape, C Shape	—	4 per module
Zakharov et al. [17]	—	Omnidirectional / car mode	—	Omnidirectional, conventional	—	4 per module
Zhao et al. [18]	—	Omnidirectional	—	car, snake	—	4 per module
Parween et al. [19]	—	Differential by steered wheels	—	Straight, Chevron, Closed	—	4 per module
Karamipour et al. [20]	—	Omnidirectional	—	longitudinal and transverse adjustments	—	4 per module

in frames 14 - 16, involves the latch arm rotating to unlock the modules.

Finally, Table I summarizes existing research contributions in the field of modular and reconfigurable omnidirectional robots. This table considers key features as: modularity which describes the modules that comprise a complete robot. These modules can be units, or robots, such as differential or Mecanum. Another characteristic is the type of locomotion of modules, this is important because it indicates their capability to operate independently. Coupled locomotion refers to the type of locomotion when modules are connected. Module reconfiguration denotes the property of modules to modify some structural characteristic, as locomotion, shape or dimensions. The connection mechanism indicates if modules connect automatically or manually, this aspect is important for potential applications in self-repairing tasks. The number of actuators for locomotion is relevant in energy consumption efficiency. These features allow to establish a reference frame in the design of modular and reconfigurable robots for holonomic motion, it is possible to observe that solutions as presented by [9] and [12] offer robustness to the modularity and reconfiguration. In this sense, the proposed robot offers an alternative design that incorporates a mechanism enabling structural variation, allowing it to alternate between nonholonomic and holonomic motion depending on the task to be performed.

V. CONCLUSIONS

This paper presented a modular mobile robot, including the calculation of its kinematic model and corresponding multibody simulations. In this work Multibody simulations demonstrate that holonomic motion can be achieved by connecting and reconfiguring nonholonomic and nonhomogeneous robotic modules. Modularity is achieved through the integration of an active mechanism that rigidly connects two modules. The combination of Mecanum wheels and the male-female connectors, results in an omnidirectional robot with enhanced load and motion capabilities. Additionally, the connection mechanism allows reconfiguration, because when servomotor lifts the latch arm, the passive spherical wheel lowers providing stability in differential drive configuration. In contrast, if servomotor lowers the latch arm, the spherical wheel lifts to prevent interference with the ground in omnidirectional mode. Due to the wheel arrangement, the Inverse Jacobian matrices differ for Module I and Module II, a condition that is useful when extending the methodology to the connected modules k and $k+1$. For n modules, the Jacobian matrix is generalized in terms of the kinematic posture equations of the Mecanum wheels, where their relative positions to the robot's geometric center influence overall the motion. Simulation results showed similarity between the analytical and multibody models. This is particularly relevant because the Multibody Toolbox has demonstrated to be a robust computational tool for simulating complex systems, such as omnidirectional mobile robots. In alignment with the SDG, this work provides a platform that can be used as an educational tool for teaching programming, robotics, as well as for developing automation experiments without the need for expensive laboratories during the early stages of design. The capabilities of the coupling mechanism were validated in a physical prototype. In preliminary test it was observed that the geometry of mating connectors ensured the centering, connection, and correct operation of robot in

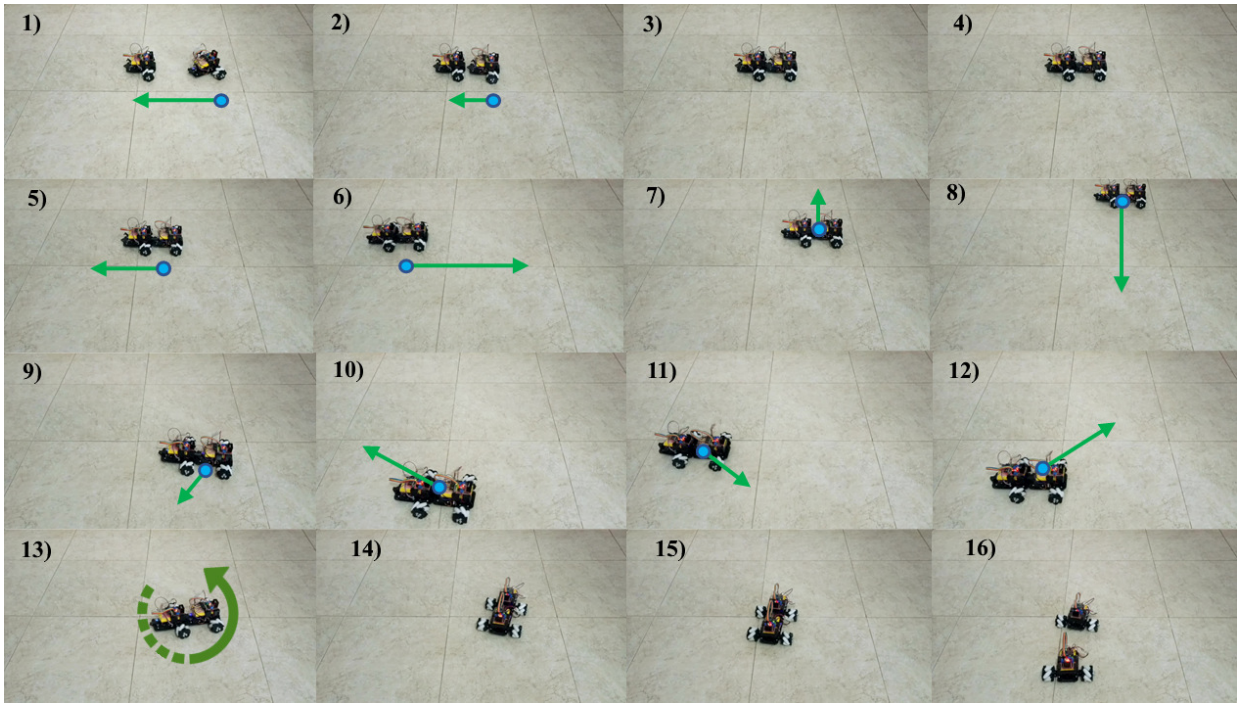

Fig. 13. Video frames of the docking and undocking process for the omnidirectional modular robot.

omnidirectional mode. However, despite the rigid connection there was backlash between modules because due to materials properties and manufacturing process. Additionally, because robot operates under open-loop control scheme, difficulties for alignment and driving modules are presented. To address these limitations, the development of a cooperative control scheme is proposed as future work to enable autonomous coupling.

ACKNOWLEDGMENTS

The authors would like to thank the Investigadoras e Investigadores por México Program of the Secretaría de Ciencia, Humanidades, Tecnología e Innovación, and the Instituto Politécnico Nacional, for their support to develop this research. Grammar enhancements and the voice used in the video abstract were generated with the assistance of AI based tools.

REFERENCES

[1] H. Ahmadzadeh, E. Masehian, and M. Asadpour, "Modular Robotic Systems: Characteristics and Applications," *J. Intell. Robot. Syst.*, vol. 81, pp. 317–357, 2016. doi: https://doi.org/10.1007/s10846-015-0237-8.

[2] M. Yim, W. Shen, B. Salemi, D. Rus, M. Moll, H. Lipson, E. Klavins, and G. S. Chirikjian, "Modular Self-Reconfigurable Robot Systems: Grand Challenges of Robotics," *IEEE Robot. Autom. Mag.*, vol. 14, no. 1, pp. 43–52, 2007. DOI: https://doi.org/10.1109/MRA.2007.339623.

[3] G. Mourioux, C. Novales, G. Poisson, and P. Vieyres, "Omni-directional robot with spherical orthogonal wheels: concepts and analyses," in *Proceedings of the 2006 IEEE International Conference on Robotics and Automation (ICRA 2006)*, Orlando, FL, USA, 2006, pp. 3374–3379. DOI: https://doi.org/10.1109/ROBOT.2006.1642217.

[4] M. Hofbaur, M. Brandstötter, S. Jantscher, and C. Schörghuber, "Modular re-configurable robot drives," in *IEEE Conference on Robotics, Automation and Mechatronics*, Singapore, 2010. pp. 150–155, DOI: 10.1109/RAMECH.2010.5513196.

[5] M. O. Tătar and C. I. Cirebea, "Modular Reconfigurable Robots," in *New Advances in Mechanism and Machine,* in *Science*, I. Doroftei, C. Oprisan, D. Pisla, and E. C. Lovasz, Eds., vol. 57. Cham, Switzerland: Springer, 2018, pp. 291–299. doi: https://doi.org/10.1007/978-3-319-79111-129.

[6] Z. Liu, M. Yue, L. Guo, and Y. Zhang, "Trajectory planning and robust tracking control for a class of active articulated tractor-trailer vehicle with on-axle structure," *Eur. J. Control*, vol. 54, pp. 87–98, 2020. doi: https://doi.org/10.1016/j.ejcon.2019.12.003

[7] J. D. Davis, Y. Sevimli, B. R. Eldridge, and G. S. Chirikjian, "Module Design and Functionally Non-Isomorphic Configurations of the Hex-DMR II System," *ASME J. Mech. Robot.*, vol. 8, no. 5, 2016. doi: https://doi.org/10.1115/1.4032273.

[8] J. D. Davis, Y. Sevimli, M. Kendal Ackerman, and G. S. Chirikjian, "A Robot Capable of Autonomous Robotic Team Repair: The Hex-DMR II System," in *Advances in Reconfigurable Mechanisms and Robots II*, X. Ding, X. Kong, and J. S. Dai, Eds. Cham, Switzerland: Springer, 2016, pp. 619–631. doi: https://doi.org/10.1007/978-3-319-23327-7_53.

[9] R. H. Peck, J. Timmis, and A. M. Tyrrell, "Omni-Pi-tent: An Omnidirectional Modular Robot With Genderless Docking," in *Towards Autonomous Robotic Systems*, K. Althoefer, J. Konstantinova, and K. Zhang, Eds. Cham, Switzerland: Springer, 2019, pp. 307–318. doi: https://doi.org/10.1007/978-3-030-25332-5_27.

[10] Y. Li, S. Dai, L. Zhao, X. Yan, and Y. Shi, "Topological Design Methods for Mecanum Wheel Configurations of an Omnidirectional Mobile Robot," *Symmetry*, vol. 11, no. 10, 2019. doi: https://doi.org/10.3390/sym11101268.

[11] Y. Li, S. Ge, S. Dai, L. Zhao, X. Yan, Y. Zheng, and Y. Shi, "Kinematic Modeling of a Combined System of Multiple Mecanum-Wheeled Robots with Velocity Compensation," *Sensors*, vol. 20, no. 1, 2020. doi: https://doi.org/10.3390/s20010075.

[12] R. Pasumarthi, S.M.B.P. Samarakoon and M.R. Elara, "Determining optimum assembly zone for modular reconfigurable robots using multi-objective genetic algorithm," *Sci. Rep.*, vol. 15, pp. 1–12. 2025. doi: https://doi.org/10.1038/s41598-024-84637-0.

[13] C. He, D. Wu, K. Chen, F. Liu, and N. Fan, "Analysis of the Mecanum wheel arrangement of an omnidirectional vehicle," in *Proceedings of the Institution of Mechanical Engineers, Part C: Journal of Mechanical Engineering Science*, vol. 233, no. 15, pp. 5329–5340, 2019. doi: https://doi.org/10.1177/0954406219843568.

[14] G.-n. Li, M. Zeng, Y. Ma, Q. Li, and W.-k. Xu, "Design of Double-Body Car-Snake Hybrid Transformable Robot," in *39th Chinese Control Conference (CCC)*, Shenyang, China, 2020. DOI: https://doi.org/10.23919/CCC50068.2020.9188511.

[15] W. Cheah, K. Groves, H. Martin, H. Peel, S. Watson, O. Marjanovic, and B. Lennox, "MIRRAX: A Reconfigurable Robot for Limited Access Environments," *IEEE Trans. Robot.*, vol. 39, no. 2, pp. 1341–1352, 2022. doi: https://doi.org/10.1109/TRO.2022.3207095.

[16] M. Chi, S. Chang, S. Cui, Z. Li, J. Li, Z. Xia, Q. Ren, "Deformation Mechanism and Design of an Omni-directional Mobile Reconfigurable Robot," in *2024 9th Asia-Pacific Conference on Intelligent Robot Systems (ACIRS)*, Dalian, China, 2024, pp. 166-170, doi: 10.1109/ACIRS62330.2024.10684923.

[17] D. N. Zakharov, A. M. Iaremenko, D. M. Kurovskii, A. M. Kurovskii, O. I. Borisov and B. Zhang, "Development of a Mobile Reconfigurable Mecanum Robot with a Locking Device of Rollers," in *2024 IEEE/RSJ International Conference on Intelligent Robots and Systems (IROS)*, Abu Dhabi, United Arab Emirates, 2024, pp. 3553-3558, doi: 10.1109/IROS58592.2024.10801549.

[18] Z. Zhao, P. Xie, J. Wang and M.Q.H. Meng, "ODD: Omni Differential Drive for Simultaneous Reconfiguration and Omnidirectional Mobility of Wheeled Robots," *IEEE Robot. Autom. Let.*, vol. 10, no. 6, pp. 5975-5982, 2025, doi: 10.1109/LRA.2025.3564207

[19] R. Parween, M. Vega-Heredia, M.M. Rayguru, R.E. Abdulkader, M.R. Elara, "Autonomous Self-Reconfigurable Floor Cleaning Robot," *IEEE Access*, vol. 8, pp. 114433–114442. doi: https://doi.org/10.1109/ACCESS.2020.2999202.

[20] E. Karamipour, S. F. Dehkordi, and M. H. Korayem, "Reconfigurable Mobile Robot with Adjustable Width and Length: Conceptual Design, Motion Equations and Simulation," *J. Intell. Robot. Syst.*, vol. 99, pp. 797–814, 2020. doi: https://doi.org/10.1007/s10846-020-01163-7.

[21] *KUKA omniMove*. KUKA® AG. [Online]. Available: https://www.kuka.com/es-mx/productos-servicios/amr-robotica-movil-autonoma/plataformas-m%C3%B3viles/kuka-omnimove

[22] A. Rauniyar, H. C. Upreti, A. Mishra, and P. Sethuramalingam, "MeWBots: Mecanum-Wheeled Robots for Collaborative Manipulation in an Obstacle-Clustered Environment Without Communication," *J. Intell. Robot. Syst.*, vol. 102, no. 3, pp. 1–18, 2021. doi: https://doi.org/10.1007/s10846-021-01359-5.

[23] E. Tuci, M. H. Alkilabi, and O. Akanyeti, "Cooperative Object Transport in Multi-Robot Systems: A Review of the State-of-the-Art," *Front. Robot. AI*, vol. 5, p. 59, 2018. doi: https://doi.org/10.3389/frobt.2018.00059.

[24] Z. Wang, G. Yang, X. Su, and M. Schwager, "OuijaBots: Omnidirectional Robots for Cooperative Object Transport with Rotation Control Using No Communication," in *Distributed Autonomous Robotic Systems: The 13th International Symposium*, R. Groß, A. Kolling, S. Berman, E. Frazzoli, A. Martinoli, F. Matsuno, and M. Gauci, Eds. Cham, Switzerland: Springer, 2018, pp. 117–131. doi: https://doi.org/10.1007/978-3-319-73008-0_9.

[25] P. Paniagua-Contro, E. G. Hernandez-Martinez, O. González-Medina, J. González-Sierra, J. J. Flores-Godoy, E. D. Ferreira-Vazquez, and G. Fernandez-Anaya, "Extension of Leader-Follower Behaviours for Wheeled Mobile Robots in Multirobot Coordination," *Math. Probl. Eng.*, vol. 2019, 2019. doi: https://doi.org/10.1155/2019/4957259

[26] S. G. M. Hossain, C. A. Nelson, K. D. Chu, and P. Dasgupta, "Kinematics and Interfacing of ModRED: A Self-Healing Capable, 4DOF Modular Self-Reconfigurable Robot," *J. Mech. Robot.*, vol. 6, no. 4, 2014. doi: https://doi.org/10.1115/1.4028132

[27] M. D. M. Kutzer, M. S. Moses, C. Y. Brown, M. Armand, D. H. Scheidt, and G. S. Chirikjian, "Design of a new independently-mobile reconfigurable modular robot," in *2010 IEEE International Conference on Robotics and Automation*, Anchorage, AK, USA, 2010, pp. 2758–2764. doi: 10.1109/ROBOT.2010.5509726.

[28] A. Castano, A. Behar, and P. M. Will, "The Conro modules for reconfigurable robots," *IEEE-ASME Trans. Mechatron.*, vol. 7, no. 4, pp. 403–409, 2002. doi: https://doi.org/10.1109/TMECH.2002.806233.

[29] P. M. Moubarak and P. Ben-Tzvi, "On the Dual-Rod Slider Rocker Mechanism and Its Applications to Tristate Rigid Active Docking," *J. Mech. Robot.*, vol. 5, no. 1, 2013. doi: https://doi.org/10.1115/1.4023178.

[30] T. Hamid, Q. Bing, and G. Nurallah, "Kinematic model of a four Mecanum wheeled mobile robot," *Int. J. Comput. Appl.*, vol. 113, no. 3, 2015. doi: http://dx.doi.org/10.5120/19804-1586.

Fernando Lucio-Reyna received the B.Sc. degree in Mechanical engineering from Instituto Politécnico Nacional (IPN), México, in 2014. In 2019 he received the M.Sc. in Mechanical Engineering, from IPN-SEPI ESIME Zacatenco. Currently, Fernando is pursuing the Ph. D. degree in the IPN. His research interests include linear and nonlinear control design, regulation theory, robotics and mechanical design.

Ricardo Tapia-Herrera received the B.Sc. degree in Industrial Robotics engineering from Instituto Politécnico Nacional (IPN), México, in 2005, the M.Sc. and Ph.D. degrees both in mechanical engineering, from IPN-SEPI ESIME Zacatenco in 2009 and 2013, respectively. His areas of interest are fuzzy control, mechanical design, robotics, analysis, synthesis, and dynamics of mechanisms. Currently, he is visiting researcher in the IPN participating in the program of SECIHTI "Investigadores por México".

Tonatiuh Hernández-Cortés received his B.Sc. degree in robotics from Instituto Politécnico Nacional, México City, México, in 2005, and M.Sc. and Ph.D. degrees in mechanical engineering from Sección de Estudios de Posgrado e Investigación, Instituto Politécnico Nacional, in 2012 and 2016, respectively. He is currently a full professor at Universidad Politécnica de Pachuca, Zempoala, México. His research interests include control of nonlinear systems, output regulation, robotics, fuzzy systems, and real-time applications.

Israel Isaías Lizardo-Parra received a B.Sc. degree in Mechanical Engineering from the Instituto Tecnológico de Veracruz in 2017 and an M.Sc. degree in Mechanical Engineering from the Sección de Estudios de Posgrado e Investigación (SEPI) at the Escuela Superior de Ingeniería Mecánica y Eléctrica (ESIME), Unidad Zacatenco, of the Instituto Politécnico Nacional (IPN). He is currently pursuing a Ph.D. in Mechanical Engineering at SEPI-ESIME Zacatenco, IPN. His research interests include biomechatronics, mechanical design, application of control techniques to robotic systems, and numerical simulations.

Jesús A. Meda-Campaña (M'00) received the B.Sc. degree in Computer Engineering (with mention of excellence) from Instituto Tecnológico y de Estudios Superiores de Monterrey (ITESM), in Culiacán, Sinaloa, México, in 1993; the M.Sc. and Ph.D. degrees in electrical engineering from Centro de Investigación y de Estudios Avanzados del Instituto Politécnico Nacional (CINVESTAV-IPN), in Guadalajara, Jalisco, México, in 2002 and 2006, respectively. His main research interests include linear and nonlinear control design, fuzzy regulation theory, optimal control, and application of control techniques to electromechanical systems and robotics. He has been an IEEE member since 2000.